Mid- to Late- Holocene Submarine Paleoseismology in the Region of the 2004 Sumatra-Andaman Earthquake

Jason Patton 1, Chris Goldfinger 1
Jeff Beeson 1, Bran Black 1
Ann Morey 1, Morgan Erhardt 1
Amy Garrett 1, Yusuf Djardjihardja 2
1. Oregon State University, COAS, Corvallis, OR 97331 jpatton@coas.oregonstate.edu
2. BPPT, Jakarta, Indonesia

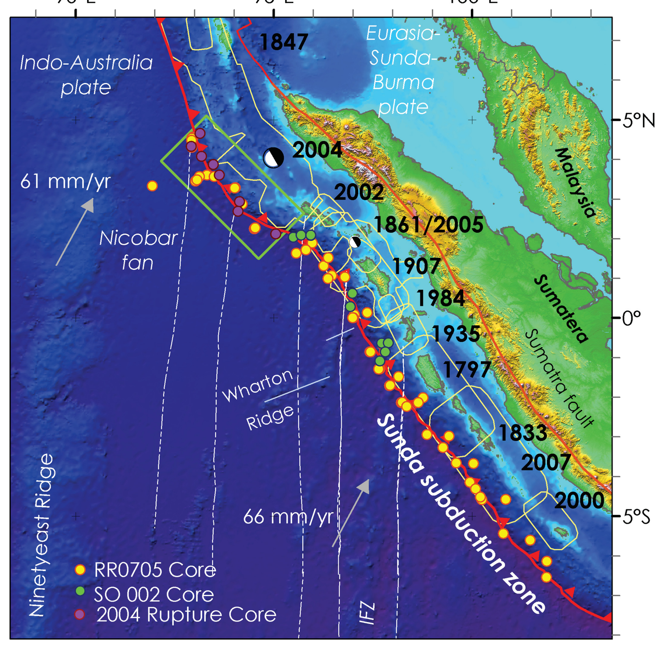

Historic ruptures, are plotted as light yellow polygons (Briggs, et al., 2006). Indo-australian plate subducts northeastwardly beneath Eurasia plate. RR0705 cores collected in 2007 are yellow dots, cores collected by NOCS in 2009 are green dots, and RR0705 cores used in this poster are purple dots. Investigator and unamed fracture zones are plotted as white dashed lines. 2004 and 2005 epicenters are also plotted. Location of map in regional correlation figure below is outlined in a green rectangle.

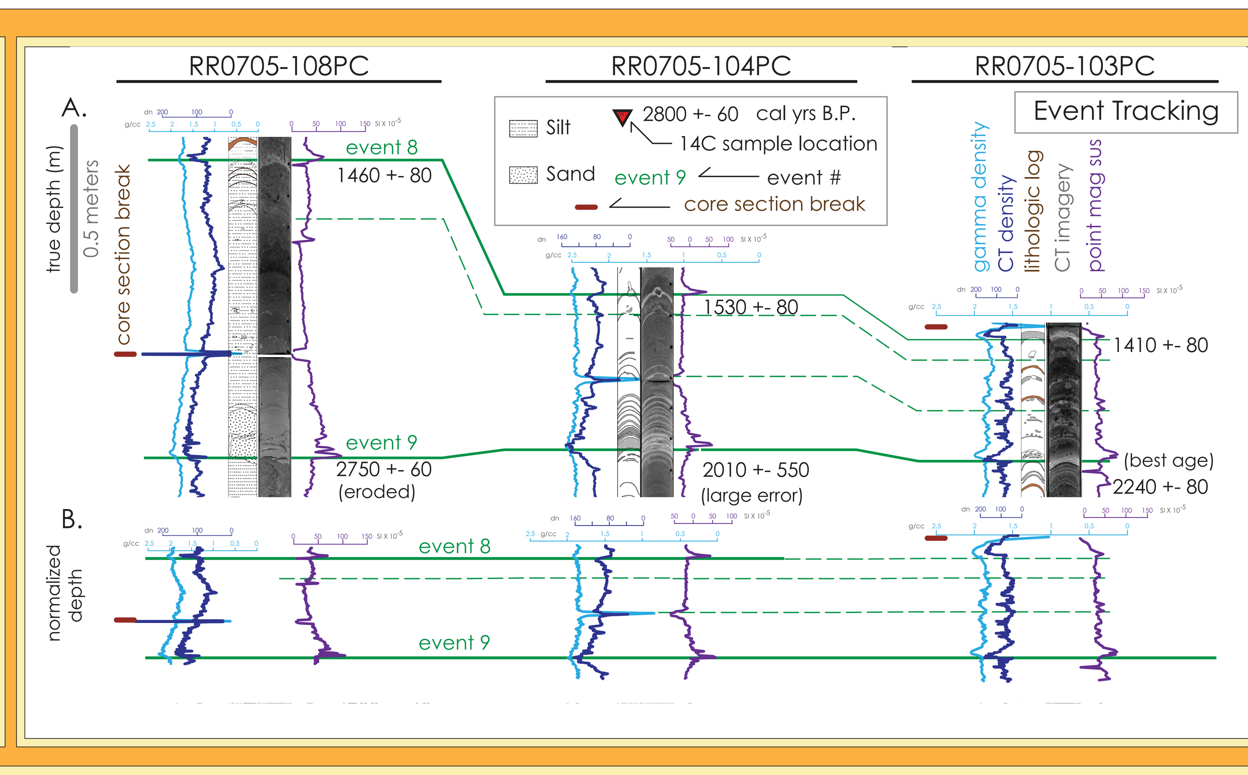

A turbidite pair (events 8 and 9) correlated between 3 slope cores with unique sedimentary sources. Entire cores are plotted below. A. From left to right, gamma density (g/cc), CT density, lithologic log, CT imagery, and point magnetic susceptibility (SI x 10-5). Cores aligned on the basal contact for event 9. Calibrated ages shown at sample locations. Core section breaks are in brown. B. Core data are plotted vs. depth, with vertical scales normalized based on stratigraphic correlations in A. Green tie lines show how data in A and B relate. Older age of event 9 in core 108PC is due to basal erosion, clearly visible in the CT data. The age of event in core 104PC has a large error due to the small sample size.

Earthquakes and tsunamis are some of the most deadly natural disasters, with the 26 December 2004 Sumatra-Andaman earthquake and tsunami responsible for the deaths of nearly a quarter of a million people. Knowledge about the earthquake cycle, through many cycles, is fundamental to understanding both the societal risk and the nature of the seismogenic process. Recurrence of great earthquakes (7 ka, years before present, BP, 1950) is estimated based on turbidite stratigraphy (representing earthquake events) correlated between 49 deep sea sediment cores in the region of the 2004 rupture. We apply criteria developed in Cascadia, Japan, and in Sumatra thus far to discriminate such events from those triggered by other mechanisms by testing the turbidite stratigraphy for synchronous triggering of turbidity currents between sedimentologically isolated basin core sites and deeper trench sites using radiocarbon, multiple proxies and ash stratigraphy.

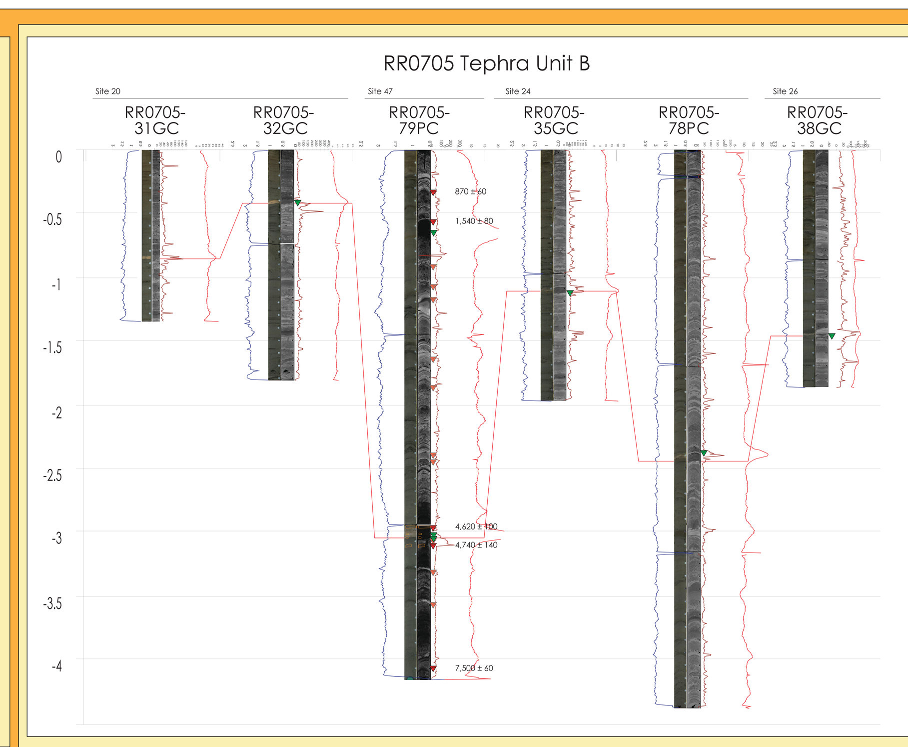

Fifteen tephra layers, varying in thickness from a few millimeters to ~5 cm, cored along the Sunda trench near Sumatra have been identified and analyzed for size, morphology, and geochemical signatures. These tephras are invaluable for stratigraphic correlation. Unit B is correlated here in six cores, just south of the 2005 rupture region in the area of the 1935 earthquake. Age control for this tephra is tightlty constrained to between 4620 +-100 and 4740 +- 140 cal yrs BP.

Glass shards from the tephra layers show systematic variations in size (30 - 200 μm) and morphology (vesicular or non-vesicular). In total, 580 glass shards (avg. 32/sample) were analyzed for major element concentrations using the Cameca SX-100 electron microprobe (EMP) at Oregon State University. Of these glass shards 359 were analyzed for trace element concentrations by LA-ICP-MS in the W.M. Keck Collaboratory for Plasma Spectrometry at Oregon State University using a newWave DUV 193 μm ArF Excimer lase and VG PQ ExCell Quadropole ICP-MS.

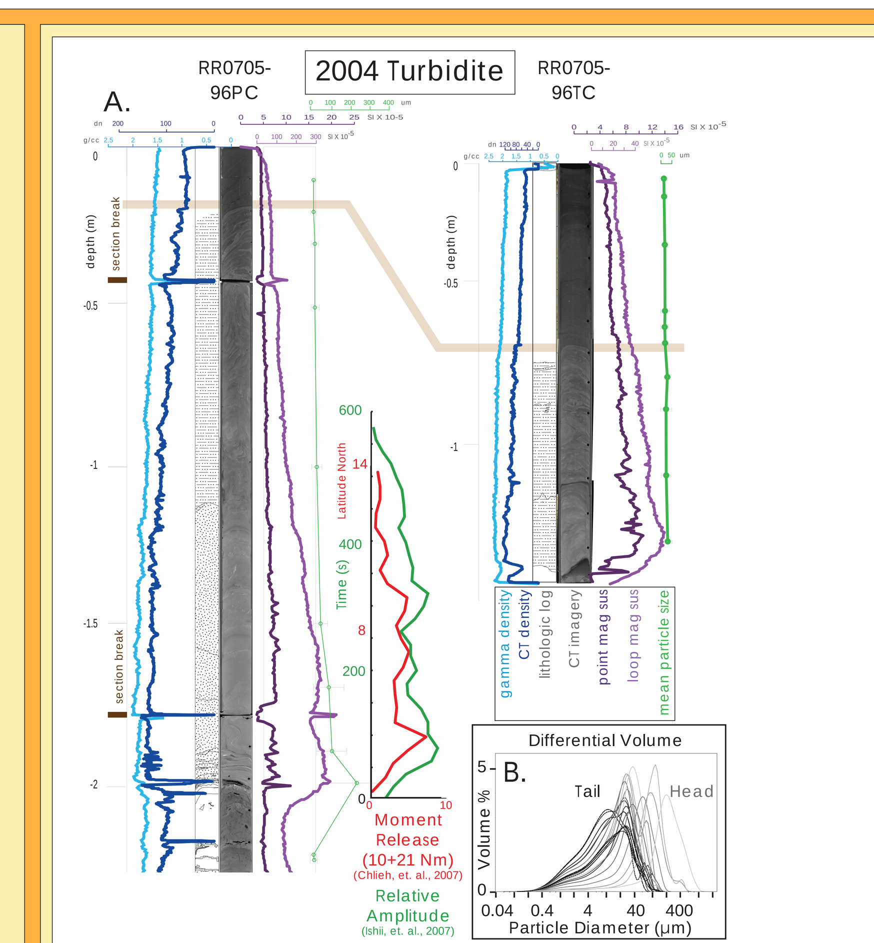

The 2004 turbidite is displayed in this figure from cores 96PC and 96TC. A. From left to right, the data shown are: Gamma density (g/cc), CT density), lithologic log, CT imagery, point and loop magnetic susceptibility (SI x 10-5), and mean grain size (μm, linear scale). Moment release (vs. latitude) in red and relative amplitude (vs. time) in green are scaled to match peaks in the loop mag sus data. A light brown tie-line connects the two data sets at a lithologic contact. Particle size distribution data from sample locations found in A are plotted by volume (%) vs. particle.

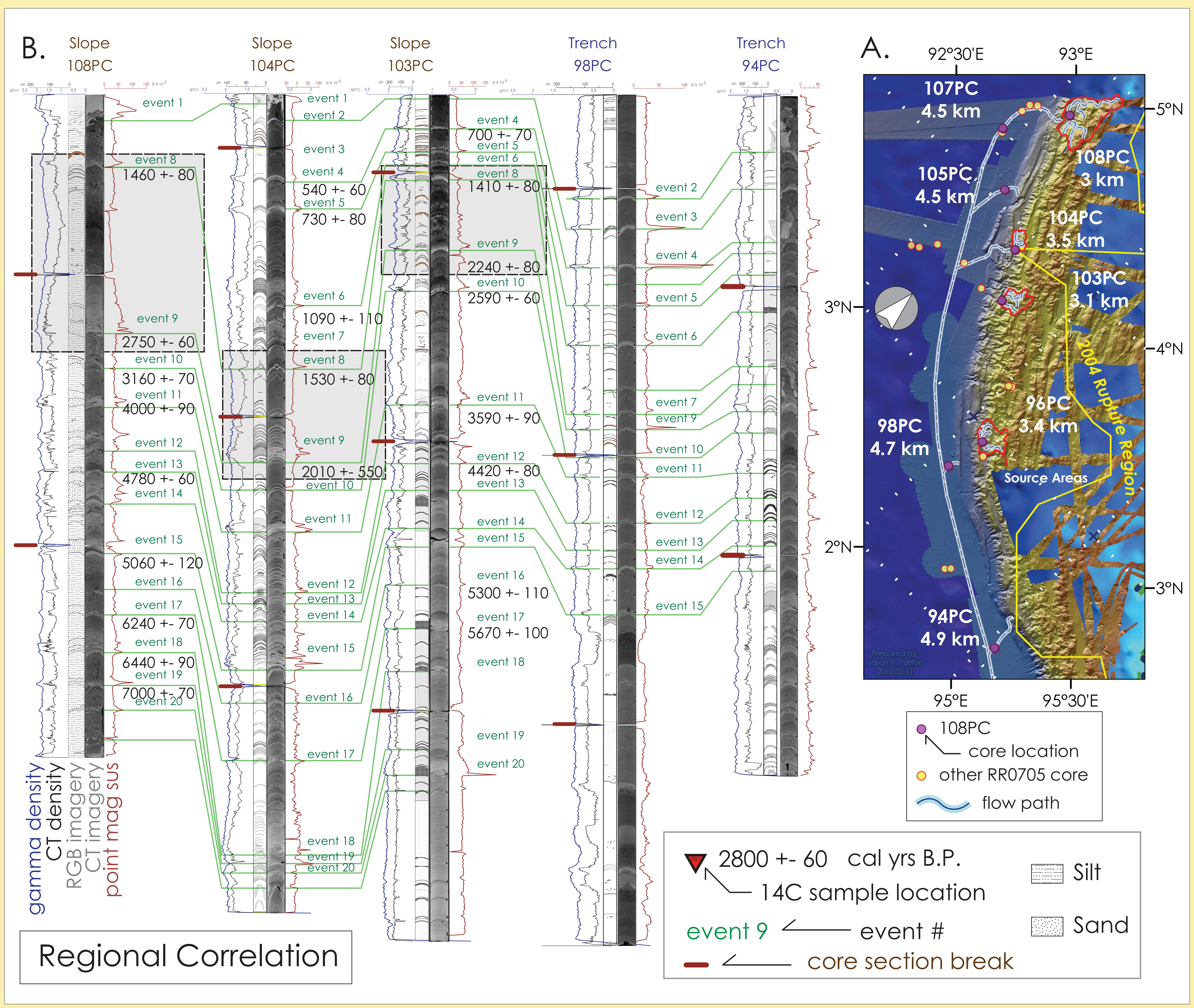

Regional stratigraphic correlations and source areas. A. Core locations (purple and yellow dots) a plotted marked with their depth on bathymetric map also showing key channel flow paths (light blue) to eight core sites. Some of the slope basins are sedimentologically isolated as shown with red. While the region that drains to core 104PC then drains to the trench, the three other slope basins are internally drained. Chlieh, et al. (2007) 2004 slip estimate is outlined in yellow. B. Stratigraphic correlations between key cores using lithology, CT, physical property and 14C data. Slope cores labeled brown; trench cores labeled blue. Location of stratigraphic details in above event tracking figure are outlined by shaded rectangles for events 8 & 9 (cores 108PC, 014PC, and 103PC).

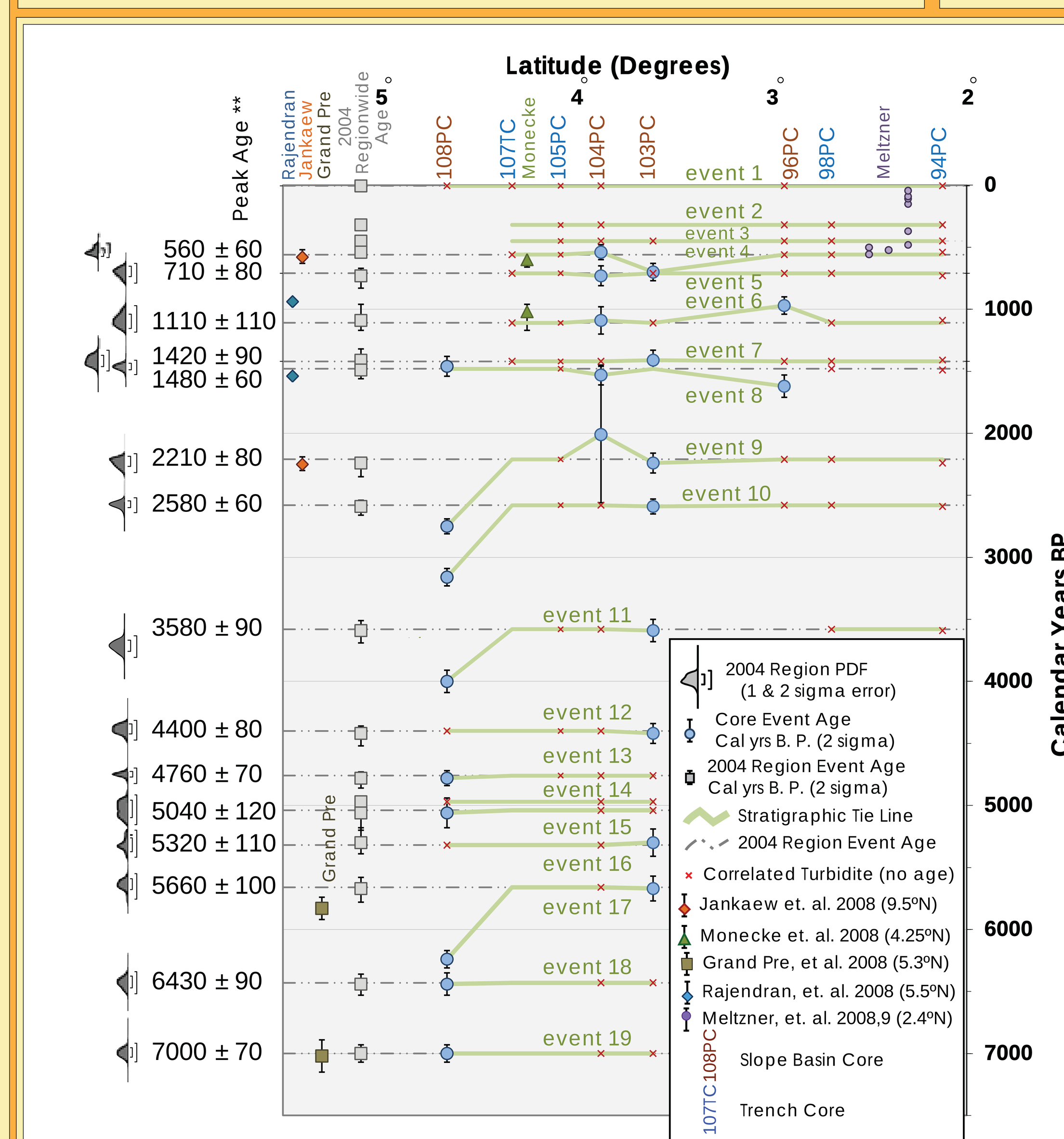

* Single ^{14}C age calibrated and reported according to Stuiver and Reimer (1998) calculated using marine reservior correction (ΔR = 16 ± 11). Errors reported to 2 standard deviations.
Probability Density Function (PDF) of combined event ages; errors reported to 1 & 2 standard deviations.
** Peak age selected from peak of PDF for each event. Error is reprted to 2 standard deviations.
¥¥ OxCal v4.1.3 Bronk Ramsey (2009); r:5 Marine data from Reimer et al (2009)

Space-Time relations for stratigraphy cored in the 2004 rupture region. 14C ages are plotted as blue circles with 2 sigma ranges. Ages are in calendar years before present (1950). Green tie lines show stratigraphic correlations. Region-wide events are designated by a dashed grey line and labeled with peak ages on the left margin with probability density functions. Correlated events without age control are designated by red x marks.

Terrestrial paleoseismic data shown with orange diamonds (paleotsunami, Thailand, not plotted vs. latitude), blue diamonds (paleotsunami, Sri Lanka, not plotted vs. latitude), brown squares (paleotsunami, Sumatra, plotted vs. latitude), green triangles (paleotsunami, Sumatra), and purple dots (coral head geodesy, Simeulue). 2004 earthquake extends beyond the latitudinal extent of this figure (Chlieh, et. al., 2007); note location map for extent.

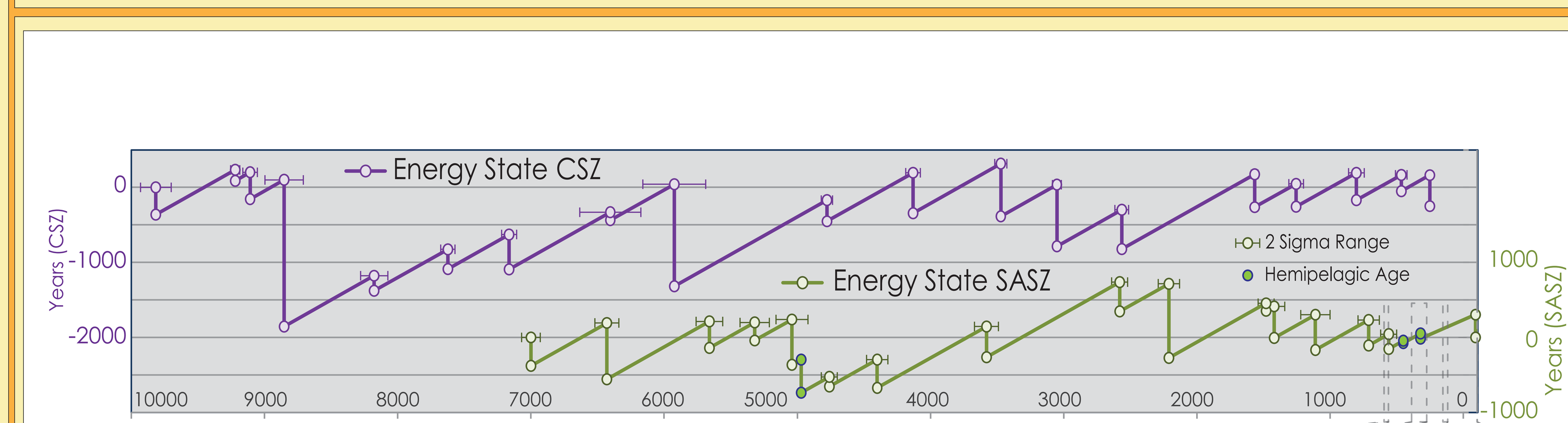

Like the comparison of moment rates to plate convergence, we evaluate long term energy cycling using plate convergence rate as a measure of strain accumulation and deposition of turbidite mass as a proxy for energy dissipation. The plate coupling ratio is assumed a value of one, likely incorrect, but a necessary approximation. The energy state is also assumed to have zero net gain/loss as a boundary condition. We do not know the transfer function between mass and seismic moment, so this is currently a relative scale. This analysis suggests that the subduction zone has variable behavior. Some events appear to release less while others appear to release more energy than available from plate convergence (slip deficit). Those that release more may have borrowed stored energy from previous cycles.

Energy state for Cascadia is in purple and Sumatra 2004 region is plotted in green. Turbidite mass is converted to years of convergence, so the vertical drops are that event's turbidite mass scaled to years. X-axis units are calendar years before 1950, so the 2004 and 2007 (Sieh data) earthquakes plot to the right of zero. Hemipelagic based age estimates are green dots without a 2 sigma range. Sieh, et al. (2008) supercycles are scaled and correlated to the energy state plot with dashed grey tie lines.